Design considerations for the hunting and braking performance of Maglev vehicle utilizing permanent magnet EDS levitation system

Karoly Kehrer, Volus Mc Kenna
Hall Industries, Inc., 514 Mecklem Lane Ellwood City PA, USA, Tel: (001 724 752 2000)
kkehrer@hallind.com

Robert Kratz
General Atomics, 3550 General Atomics Court, San Diego, CA 92121-1122 USA, Tel: (001 858 455 3000)
Robert.kratz@gat.com

ABSTRACT: The Urban Maglev Vehicle levitated by Permanent Magnet Electrodynamic Suspension system (EDS) and propelled with Linear Synchron Motor (LSM) requires a new type of design that is adapted to the technology and guideway configuration. A matured urban terrain can only be served with a highly flexible, articulated car-body structure. To establish adequate design requirements for the vehicle, the effect of flexible units on the overall ride performance needs to be analyzed. One major concern of magnetically suspended cars is hunting, a phenomenon of a self-excited lateral oscillation with a certain wavelength and amplitude that is coupled to the forward speed of the vehicle. In rail operation it is determined by the wheel-rail restoring forces (caused by the conicity of the wheel-rail-contours) and friction-creep characteristics of the wheel-rail contact. The EDS suspension in turn has minimum damping and the restoring forces are evenly distributed. To understand the combined effect of these basic differences, the magnitude of the available restoring forces and their relation to the vehicle structure is investigated. The paper is aimed to clarify the behavior of these forces as a function of the vehicle movement relative to the reaction and propulsion rails, with emphasis on the nonlinear magnetic lateral stabilization forces, the nonlinear primary magnetic vehicle suspension and propulsion characteristics.

1 INTRODUCTION OF THE SYSTM ARCHITECTURE

The general arrangement of the Urban Maglev vehicle and the supporting guideway is represented on the computer rendering bellow.

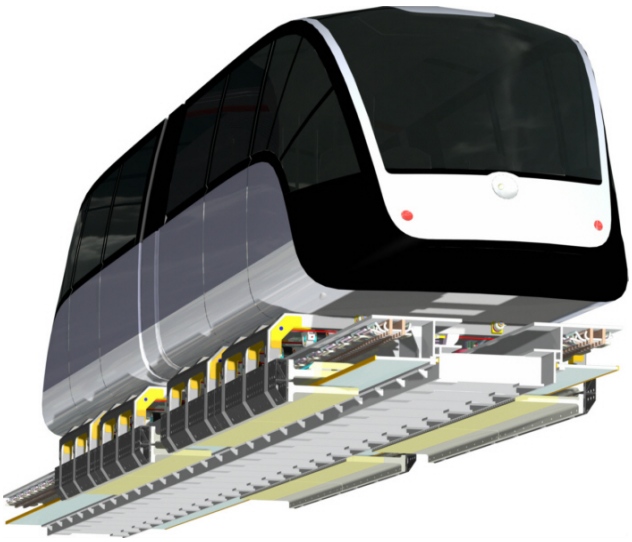

Figure 1: base line vehicle

The picture shows the base line vehicle. Two modules are connected by an articulation unit and are supported by two levitation structures (chassis). The chassis are equipped with double sided levitation Halbach arrays and drive arrays. The Linear Synchron Motors are mounted beneath the guideway top plates.

The next picture shows the test vehicle on the guideway in operation. It represents one vehicle body module and is supported by one chassis module.

Figure 2: test vehicle

The interrelation between the levitation and propulsion magnet arrays and the guideway can be summarized on the close-up photograph of the test chassis. The Litz Wire Reaction Rail is straddled by the double arrays. The

top member of the array carries two rows of propulsion magnets whose field locks into the traveling wave being generated by the Linear Synchron Motor. Lateral stability is provided by the attraction forces between the propulsion magnets and the iron core of the motor winding and the d-component (I_d) of the drive current.

Figure 3: Levitation/propulsion close-up

2 SIMILARITIES AND DIFFERENCES BETWEEN LEVITATED AND RAIL SUPPORTED VEHICLES

In order to utilize the wealth of knowledge accumulated over one and a half a century, it is useful to highlight the similarities and basic differences between rail supported and levitated systems. First, the purpose of both is the same: move people from one place to another fast, economically and comfortably. Therefore the payload is similar; usually 50 to 150 persons per car, 3.5 to 10 tons unevenly distributed and unsecured "cargo". Also, one can find the speed range to be comparable with the Urban Maglev operating speed (80 to 160 km/h), although, the levitated system offers the most advantages at the high end of the speed spectrum. Turn radius for urban deployment has to be the same, about 18 m. If the transportation is designed for urban areas, the advantage of the levitated system will be the higher speed, which can be attained at considerably lower noise level due to the lack of surface contact and to the magnetic propulsion with no moving parts.

However, the differences between operational characteristics are significant. The primary spring constant for rail-wheel contact can be considered "infinite" in comparison to that of primary and secondary suspension components and to the magnetic support as well, while, for levitated vehicle is only 66,000 N/mm. Lateral restoring force for a 20 ton vehicle is ~25 kN. In comparison the rail-wheel conicity provides in the excess of 35-60 kN on a typical curved track of a few hundred meter radius. Although the most significant difference is that the later figure represents concentrated force while the magnetic restoring force is being evenly distributed along the length of the vehicle support magnets.

3 LATERAL RESTORING FORCES OF THE URBAN MAGLEV VEHICLE

The main contributor to the lateral restoring forces for the permanent magnet levitation is the passive attractive force between the propulsion magnets and the LSM iron rail. It is a function of the gap, **g3** as denoted in F*igure 4*. The diagram below shows the change of this force as a function of two variables: vertical gap and lateral displacement of the magnets relative to the iron rail. For operational stability it is an important function and the calculations were carefully verified using the data of a full-scale simulation.

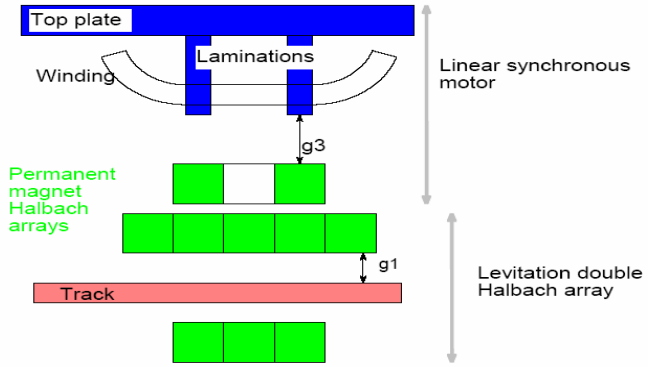

Figure 4: Levitation propulsion scheme

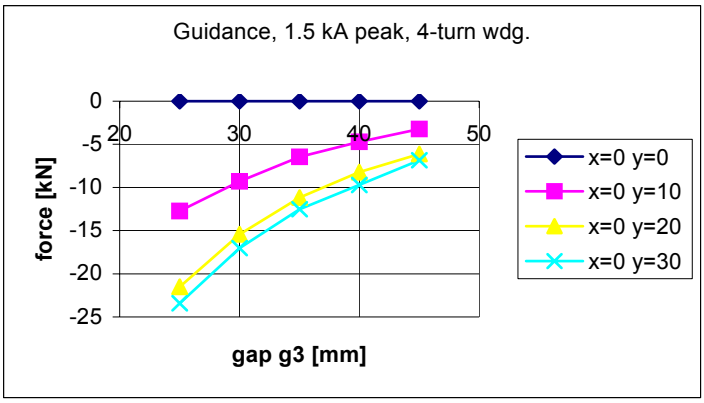

Figure 5 Restoring forces as function of the vertical gap, g3 and lateral displacement

The active attractive force generated between the LSM coils and the propulsion magnets is a function of four variables, the two gaps, g3 and Δ_y, the forward position of the propulsion array relative to the peak thrust position and the current rate.

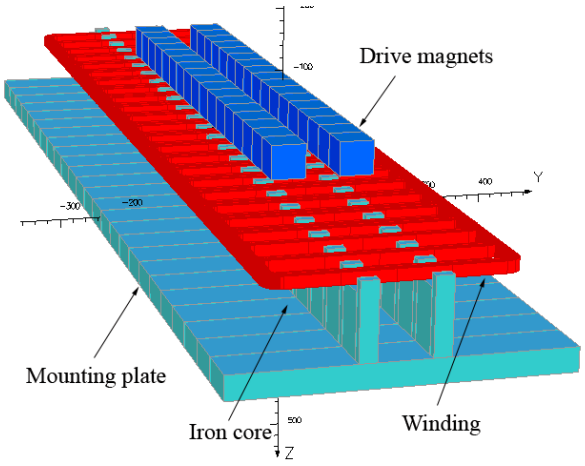

Figure 5-1: The complimentary view of the LSM arrangement (show upside down for visibility)

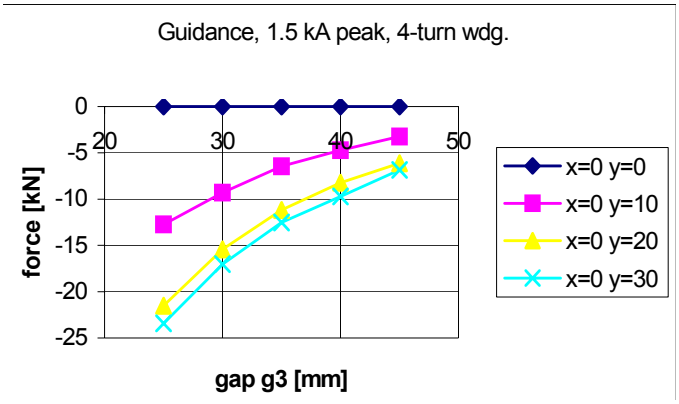

Figure 6: Restoring forces as function of of the drive current, vertical gap g3 and lateral displacement, Δy.

The active lift portrays a sinusoidal change with the change of the forward position.

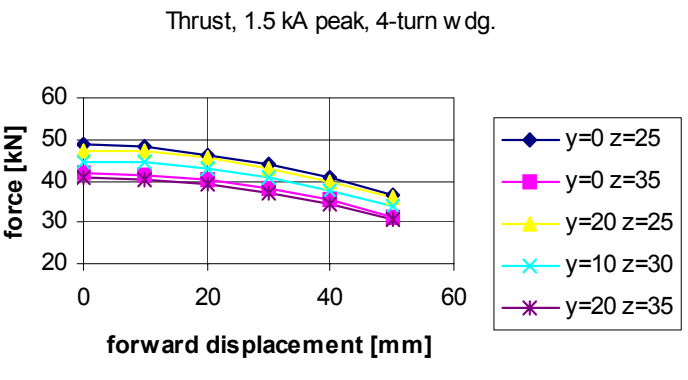

Figure 7: Restoring forces as function of the drive current, vertical gap, g3 lateral displacement, Δy, and forward displacement $\Delta_{x..}$ (From $\Delta_x = 0$ the active lift force contribution follows a sin-function with good accuracy.)

Lateral movement of the levitated vehicle is limited by guide wheels. This arrangement essentially provides the same protection as does the wheel flange for the railcar. The only difference is that the lateral wheels cannot climb the levitation substructure, nor they can overturn it.

The nominal clearance for the guide wheels is 50 mm on each side. The restoring force has its peak value at approximately 25 mm lateral displacement. Beyond that limit it gradually falls as the gap gets wider between the magnets and the rail.

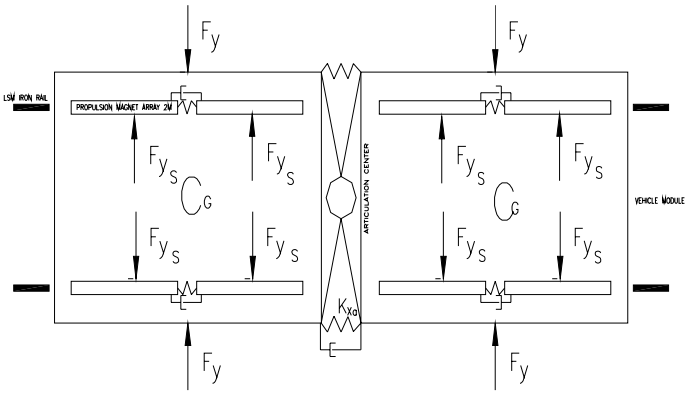

Figure 8 Restoring forces on tangent guideway

As it has been noted, the lateral forces unlike the rail vehicle restoring forces are evenly distributed along the full length of the levitation magnet arrays; therefore the resultant vector can be represented at the geometrical center of the levitation magnet arrays as is shown in the sketch above.

4 HUNTING OF THE LEVITATED VEHICLE EQUIPPED WITH ARTICULATION

Forces acting on a articulated vehicle traveling on a level tangent track are the propulsion forces generated by the interaction between the LSM and the propulsion magnet arrays, the drag forces, the viscous forces, wind forces and uneven distribution of the passenger load that can move freely, thereby causing the random migration of the centers of gravity during operation. Lastly, the allowable irregularities of the guideway structure provide a stochastic input in both vertical and lateral directions and are the constant unavoidable sources of initial disturbances.

Further disturbances on the curved track are caused by the centrifugal forces and the partial de-synchronization of the two Linear Synchron Motors. The geometrical de-synchronization of the two LSM motors results in different phase angles on the two sides that correspond with different propulsion forces. The resulting couple is trying to turn (yaw) the vehicle module around the z axis.

The roll, pitch and yaw motion changes the levitation and motor gap and the drag along with the propulsion forces coupled to it. The diagrams below provide the representative range of the drag force changes as a function of gap and forward velocity over the Litz wire reaction rail and over the eddy current emergency braking sections.

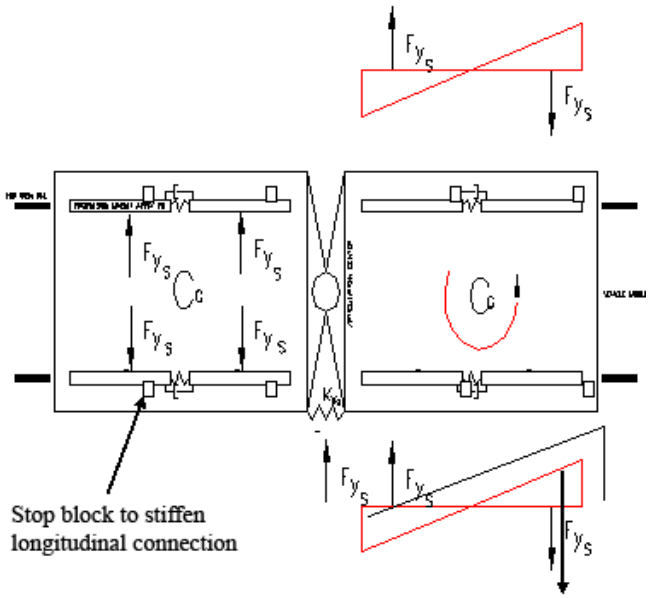

Figure 9: Static model of an articulated vehicle. The supporting levitation structures are connected with an articulation unit through the body modules.

The uneven drag forces acting on the left and right levitation arrays form a couple and tend to rotate the module around its z-axis. This unwanted effect is worsened by the fact that on the opposite side the propulsion forces are increasing too due to the closure of the motor gap, g3. The attraction between the LSM iron rail and the propulsion magnets creates a triangularly distributed lateral restoring force, whose two resultants also creates a couple rotating the body around the z-axes to the opposite direction. If the two articulated modules were separated, i.e. no lateral force were transmitted from the front to the rear module, the center of rotation would more or less coincide with the center of gravity of that unit. The articulation, by its nature transmits forces not only in lateral but in all three directions (x,y,z). As a result the axis of rotation of the front unit migrates backwards toward the articulation pivot point.

This backward migration of the rotation point has a stabilizing effect, for the distance between the resultant restoring force and the rotation point is increasing.

In the case of laterally damped articulation structure the characteristics of the damper, $C_{ARTICULATION}$, can modify the effect of mass damping and the position of the rotational center of the trailing unit.

The gap difference between the left and right side of the vehicle is a function of the magnetic spring constant, that under normal operating conditions limits the vertical heave or roll movement to ~2-3 mm. The following diagram shows the resulting force differences when the nominal levitation gap closes in on one side and opening on the other.

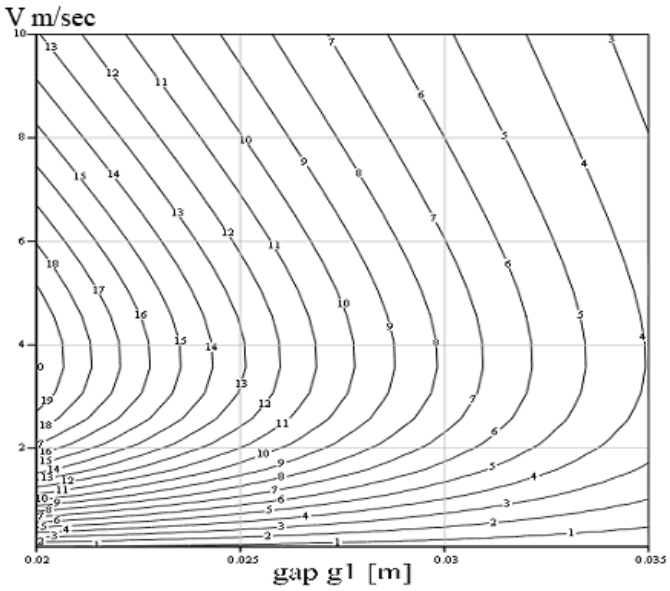

Figure 10: Drag force of the Litz track on one levitation structure

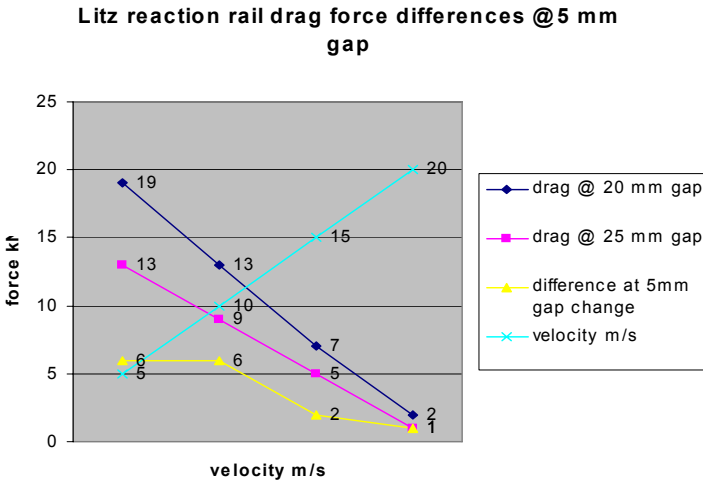

Figure 11: Shows the different of the drag force

The possible maximum drag force differences between the left and right side occurs when the vehicle enters the emergency braking section of the levitation rail.

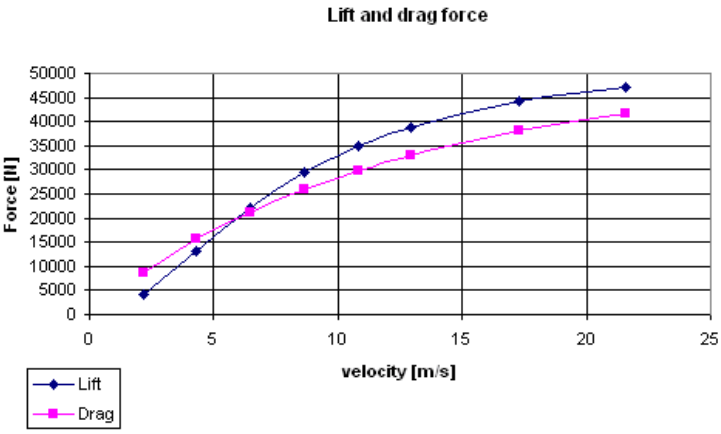

Figure 12: Lift and drag force of the double plate system at a gap g_1 = 27 mm. Both plates are 6 mm thick, 25 MS/m. Forces are for the test chassis with 2 levitation skis.

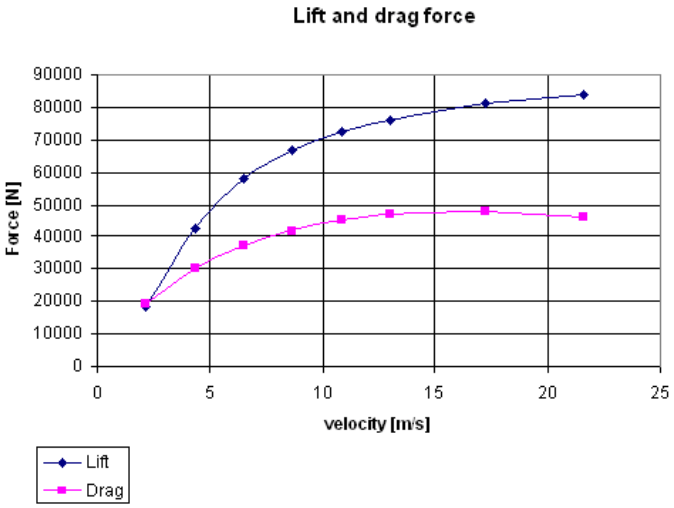

Figure 13: Lift and drag force of the double plate system at a gap $g_1 = 22$ mm. Both plates are 6 mm thick, 50 MS/m. Forces are for the test chassis with 2 levitation skis.

The two diagrams above assume 5 mm gap difference from side to side. The next diagram depicts the result as a function of velocity.

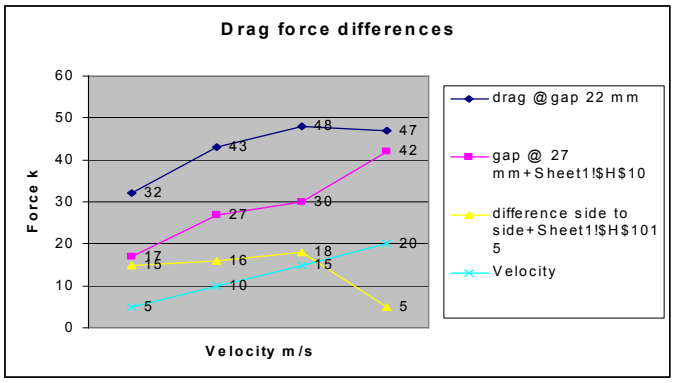

Figure 14: Drag force difference from side to side over the braking section

These rather high values may result in violent contact between the guideway and lateral wheels, although this only can happen in an emergency scenario when a vehicle has lost control and enters the safety brake zone.

The major cause of hunting for a rail-supported vehicle is the velocity dependence of uneven creep forces experienced by the right and left wheel. As the wheelset moves to the side the rolling radius grows on one side and shrinks on the other due to the conicity of the thread. As a result, one wheel has to turn faster than the nominal RPM, the other turns slower. Since the wheels are rigidly attached to the axle, creep forces develop at the wheel rail contact path and the forward component of the creep force forms a couple that turns the wheelset around its z-axis.

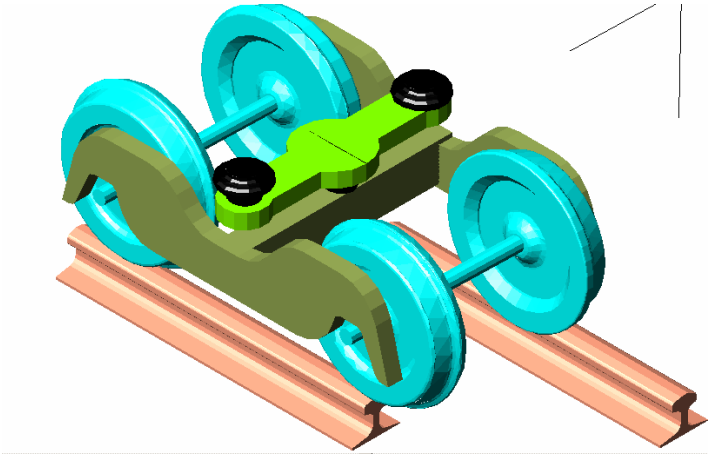

Figure 15: Conventional three piece rail truck

The component of the normal force acting on the conical surface of the thread creates a lateral restoring force, causing the wheelset to move and yaw in the opposite direction. As the forward velocity, **v** increases, both the restoring forces and the frequency of the resulting yaw of the wheel are changing. The wheelset over-shoots more and more, and at, or above the critical forward speed, $\mathbf{v}_c$, the origin loses its stability and moves to an isolated closed trajectory.

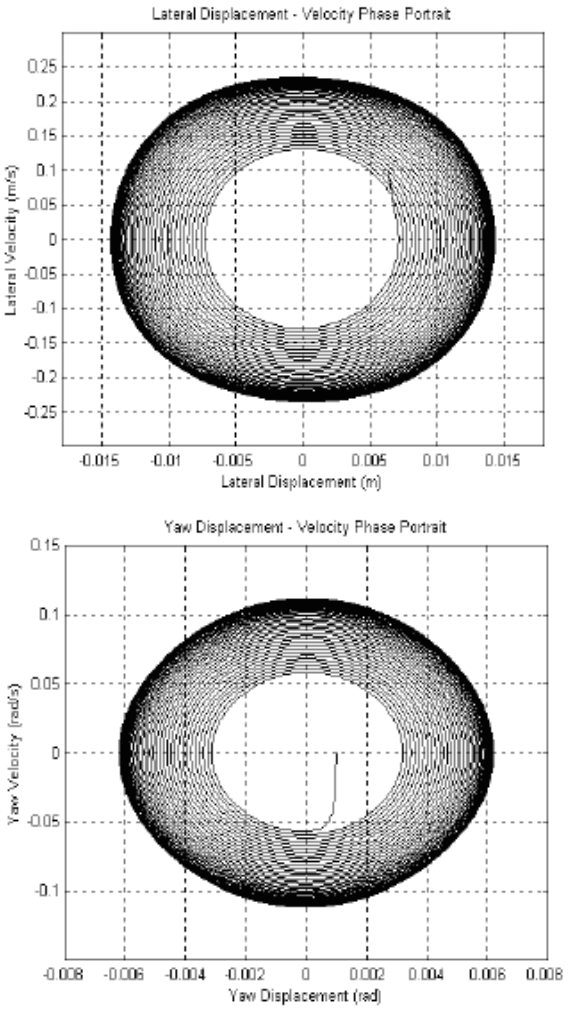

Figure 16: Phase portrait of the lateral and yaw displacement

And, as it is passing the bifurcation point, the system exhibits a self-sustained oscillation.

It is important to note that larger conicity (λ) corresponds to lower critical forward velocity, for the critical velocity is inversely proportional to the square root of lambda.

There are significant similarities and differences in the behavior of a levitated array and a wheeled rail truck. As the magnetically levitated vehicle rolls on tangent guideway (track) its levitation arrays experience different magnitude of drag force on the two sides of the vehicle as a result of the difference in the levitation gap, g1. In addition, on tangent guideway the LSM propulsion force will also vary as a function of the gap. If the LSMs on the two sides are not independently controlled, the vehicle experiences different propulsion forces on the inside and the outside drive coils on the curved guideway, due to the partial de-synchronization between the Linear Synchron Motor and propulsion array's wavelength.

The roll movement, which is induced on the car body and on its supporting levitation structure by inputs of track irregularities, centrifugal forces, passenger movement, and wind gusts, becomes the primary cause of the possible hunting. An additional source that contributes to the hunting is the LSM propulsion whose propulsion force is also changing from side to side as the levitation gap, g1 and its coupled counterpart the propulsion gap, g3 is changing.

The possible cause of hunting is the velocity dependence of the roll frequency.

$$\ddot{x}m - \dot{x}c - xk = F(t)$$

The nature and the effect of the restoring forces are significantly differing from that of wheeled vehicle. As the array yaws, it opens up the lateral gap between the LSM iron rail and propulsion magnet creating a lateral component, F_y a magnetic attraction between the LSM iron rail and the propulsion magnet arrays. This F_y component is the major contributor to the restoring forces and acts as it is shown below.

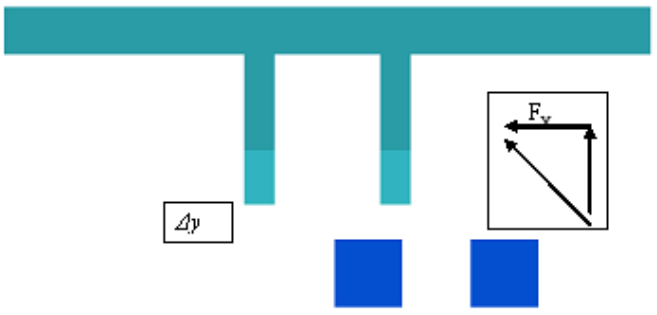

Figure 17: The propulsion magnet array's lateral displacement, Δy, relative to the iron rail

The diagram below shows the restoring force as a function of the lateral gap.

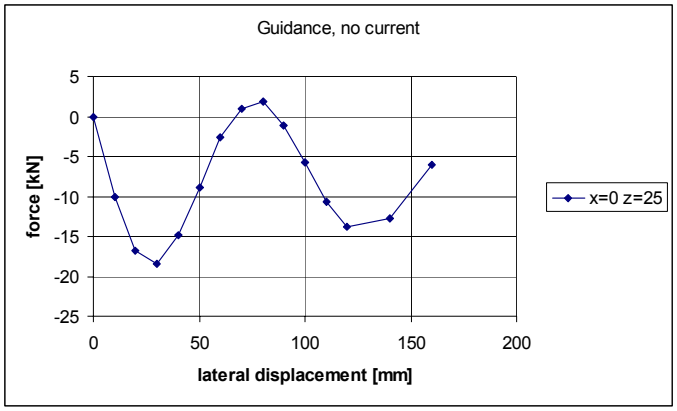

Up to ~ 25 mm displacement in the Y direction the change of forces is close to linear

Figure 18: Measured lateral restoring force

The forces on the permanent magnets or on the iron-coil-system are found by integration of the Maxwell stress tensor over a surface enclosing the permanent magnets structure. A series of calculations were performed, where the levitation array was shifted from the central position. There was no current in the LSM windings; the calculated forces are thrust (which should be 0), passive lift and guidance from the iron rails. The calculations were performed for a two-wavelength (~800 mm) levitation array. Since the full vehicle have a total of 36 wavelengths, by multiplying by 18 the estimate for a full vehicle can be obtained. The propulsion current variation from 500 A to 3000 A (peak) has little or no effect on the lateral restoring force.

The yaw movement of the levitation structure results in small angular displacement, ψ, for the lateral movement on tangent guideway is physically limited by the lateral guide wheels and by distance between these wheels. The maximum lateral displacement is 50 mm, the distance is 3.8 m, therefore the resulting angle is extremely small, 0.0132 radian. As figure 18 shows, the lateral restoring forces within this range are linear.

Once the roll movement generates yaw rotation, thus opening the lateral gap (Δ_y), the passive lift component of the propulsion array is decreasing and, at the same time, the propulsion force is decreasing too. The effect on the thrust loss as a function of the actual propulsion gap, g3 is shown on the diagram (Figure 19).

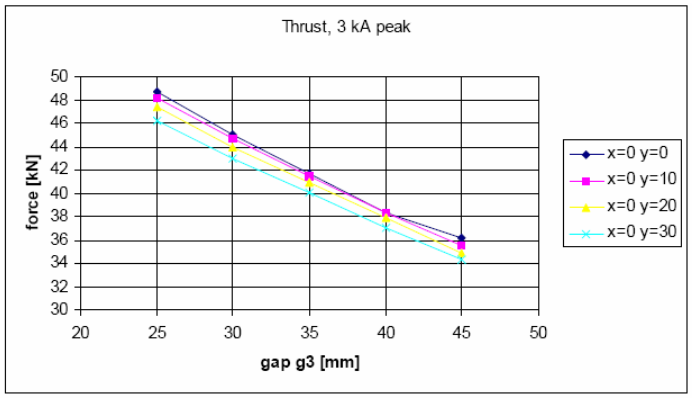

Figure 19: The change of trust as a function of propulsion gap, g3 at different lateral displacement values. (Full vehicle, two levitation structure is calculated.)

As long as the lateral displacement, (Δ_y) does not exceed a 20 mm range, it has no significant effect on the propulsion. However, differences (5-6 mm) in the vertical gap, g3 between the two sides can create 8 kN unbalanced force in addition to the 2 x 6 kN difference in drag force at low speed. These calculated and verified figures for an articulated base line vehicle result in 20 kN destabilizing forces.

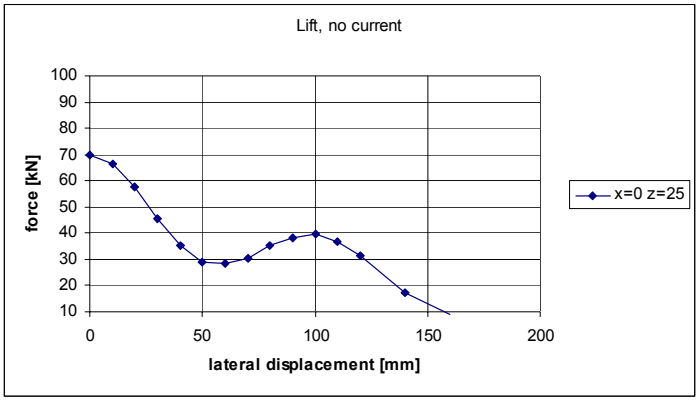

Figure 20: Change of the passive lift force as a function of lateral displacement (Δ_y)

Another significant contributor to the uneven forward forces is the change of propulsion force as a function of the phase angle, which changes as the vehicle negotiates curves.

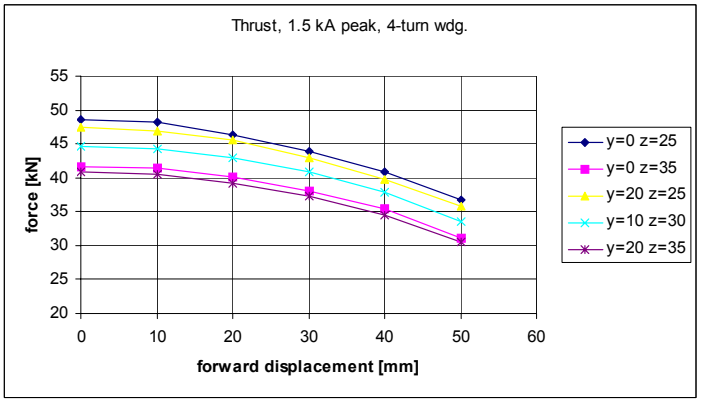

Figure 21: Trusts as a function of the motor phase angle (forward displacement)

The lateral equation of the levitation structure is:

$$F_{PROPYL}+F_{PROPYL}+F_{DYL}+F_{DYR}+F_{SUSP}-m_{LT}\,g\Phi=m_{LT}\ddot{y}_{LT}$$

F_{DYi} lateral component of the drag force left L and right R

F_{PROPYi} lateral component of the prolusion force left L and right R

F_{SUSP} suspension forces

m_{LT} mass of the levitation structure

Φ roll angle

$\ddot{y}_{LT}$ lateral displacement /acceleration

The yaw equation for the levitation structure is:

$$I_{LTZ}\,\ddot{\psi}_{LT}=-I_{LTY}\,\dot{\Phi}-a(F_{DXL}-F_{PROPXL}-F_{DXL}-F_{PROPXL})+M_{SUSPLTi}$$

$I_{LT\,Z}$ Rotational inertia of the levitation structure around the z-axis

ψ_{LT} Yaw angle

I_{LTY} Rotational inertia of the levitation structure around the y-axis

Φ Roll angle

a Half of the gauge

F_{DXi} Drag force in the longitudinal direction left and right

F_{PROPXi} Propulsion force in the longitudinal direction left and right

$M_{SUSPLTi}$ Roll and yaw suspension moments around the x- and z-axes respectively

For small angels cos (Φ and ψ) are replaced by Φ and ψ respectively. The levitation magnet arrays have substantially higher mass m_{LT} than a single wheel-set therefore provides higher mass damping.

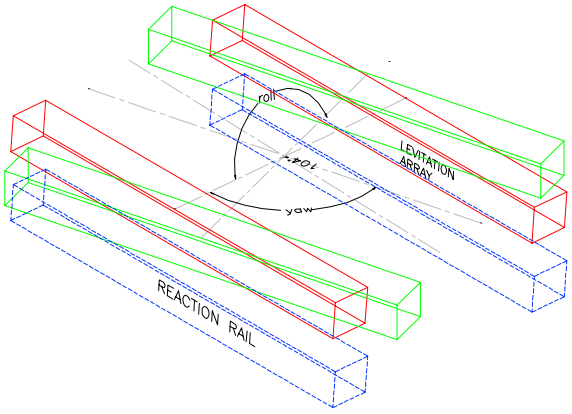

Figure 22: Yaw and roll angles of the levitation array (Green). Parallel with the reaction rail the normal position of the levitation array is shown in red. The displacements in both direction, Δ and g,1 are exaggerated for visibility.

Based upon the investigations and full-scale test verifications of the calculations, the connection between the levitation structure and the car body was designed and built to provide high longitudinal stiffness using stop block to connect the two structures. The relative angular movement between the levitation structure and the car body is controlled by an adjustable lateral air springs and magneto-rheological dampers. Similarly, to limit roll, the vertical air springs are also controlled. The adjustability of the vital components identified by the study permits the evaluation and the fine tuning of the test vehicle, thereby assists the engineers to refine the design.

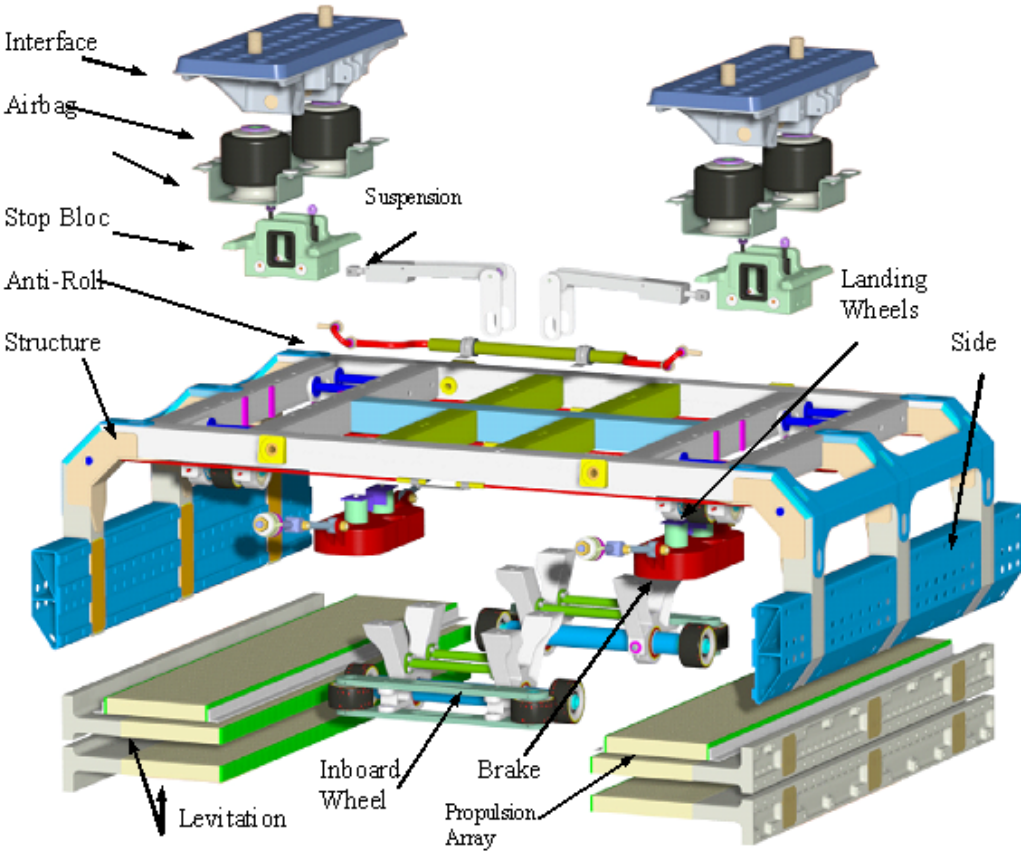

Figure 23: Exploded view of the levitation structure